

# Altered global signal topography in Alzheimer's disease

Pindong Chen,<sup>a,b</sup> Kun Zhao,<sup>c,d</sup> Han Zhang,<sup>c</sup> Yongbin Wei,<sup>c</sup> Pan Wang,<sup>e</sup> Dawei Wang,<sup>f</sup> Chengyuan Song,<sup>g</sup> Hongwei Yang,<sup>h</sup> Zengqiang Zhang,<sup>i</sup> Hongxiang Yao,<sup>j</sup> Yida Qu,<sup>a,b</sup> Xiaopeng Kang,<sup>a,b</sup> Kai Du,<sup>a,b</sup> Lingzhong Fan,<sup>a</sup> Tong Han,<sup>k</sup> Chunshui Yu,<sup>l</sup> Bo Zhou,<sup>m</sup> Tianzi Jiang,<sup>a,b</sup> Yuying Zhou,<sup>e</sup> Jie Lu,<sup>h</sup> Ying Han,<sup>n,o,p</sup> Xi Zhang,<sup>m</sup> Bing Liu,<sup>q</sup> and Yong Liu,<sup>a,b,c,\*</sup> Alzheimer's Disease Neuroimaging Initiative<sup>f</sup>



<sup>a</sup>Brainnetome Center & National Laboratory of Pattern Recognition, Institute of Automation, Chinese Academy of Sciences, Beijing, China

<sup>b</sup>School of Artificial Intelligence, University of Chinese Academy of Sciences, Beijing, China

<sup>c</sup>School of Artificial Intelligence, Beijing University of Posts and Telecommunications, Beijing, China

<sup>d</sup>Beijing Advanced Innovation Center for Biomedical Engineering, School of Biological Science & Medical Engineering, Beihang University, Beijing, China

<sup>e</sup>Department of Neurology, Tianjin Huanhu Hospital Tianjin University, Tianjin, China

<sup>f</sup>Department of Radiology, Qilu Hospital of Shandong University, Ji'nan, China

<sup>g</sup>Department of Neurology, Qilu Hospital of Shandong University, Ji'nan, China

<sup>h</sup>Department of Radiology, Xuanwu Hospital of Capital Medical University, Beijing, China

<sup>i</sup>Branch of Chinese PLA General Hospital, Sanya, China

<sup>j</sup>Department of Radiology, the Second Medical Centre, National Clinical Research Centre for Geriatric Diseases, Chinese PLA General Hospital, Beijing, China

<sup>k</sup>Department of Radiology, Tianjin Huanhu Hospital, Tianjin, China

<sup>l</sup>Department of Radiology, Tianjin Medical University General Hospital, Tianjin, China

<sup>m</sup>Department of Neurology, the Second Medical Centre, National Clinical Research Centre for Geriatric Diseases, Chinese PLA General Hospital, Beijing, China

<sup>n</sup>Department of Neurology, Xuanwu Hospital of Capital Medical University, Beijing, China

<sup>o</sup>Beijing Institute of Geriatrics, Beijing, China

<sup>p</sup>National Clinical Research Center for Geriatric Disorders, Beijing, China

<sup>q</sup>State Key Laboratory of Cognition Neuroscience & Learning, Beijing Normal University, Beijing, China

## Summary

**Background** Alzheimer's disease (AD) is a neurodegenerative disease associated with widespread disruptions in intrinsic local specialization and global integration in the functional system of the brain. These changes in integration may further disrupt the global signal (GS) distribution, which might represent the local relative contribution to global activity in functional magnetic resonance imaging (fMRI).

**Methods** fMRI scans from a discovery dataset ( $n = 809$ ) and a validated dataset ( $n = 542$ ) were used in the analysis. We investigated the alteration of GS topography using the GS correlation (GSCORR) in patients with mild cognitive impairment (MCI) and AD. The association between GS alterations and functional network properties was also investigated based on network theory. The underlying mechanism of GSCORR alterations was elucidated using imaging-transcriptomics.

**Findings** Significantly increased GS topography in the frontal lobe and decreased GS topography in the hippocampus, cingulate gyrus, caudate, and middle temporal gyrus were observed in patients with AD ( $P_{\text{adj}} < 0.05$ ). Notably, topographical GS changes in these regions correlated with cognitive ability ( $P < 0.05$ ). The changes in GS topography also correlated with the changes in functional network segregation ( $\rho = 0.5$ ). Moreover, the genes identified based on GS topographical changes were enriched in pathways associated with AD and neurodegenerative diseases.

**Interpretation** Our findings revealed significant changes in GS topography and its molecular basis, confirming the informative role of GS in AD and further contributing to the understanding of the relationship between global and local neuronal activities in patients with AD.

eBioMedicine  
2023;89: 104455  
Published Online 7  
February 2023  
<https://doi.org/10.1016/j.ebiom.2023.104455>

\*Corresponding author. School of Artificial Intelligence, Beijing University of Posts and Telecommunications, Beijing, 100876, China.

E-mail address: [yongliu@bupt.edu.cn](mailto:yongliu@bupt.edu.cn) (Y. Liu).

<sup>f</sup>Data used in the preparation of this article were obtained from the Alzheimer's Disease Neuroimaging Initiative (ADNI) database ([adni.loni.usc.edu](http://adni.loni.usc.edu)). Therefore, the investigators within the ADNI contributed to the design and implementation of ADNI and/or provided data but did not participate in the analysis or writing of this report. A complete listing of the ADNI investigators is available at [http://adni.loni.usc.edu/wp-content/uploads/how\\_to\\_apply/ADNI\\_Acknowledgement\\_List.pdf](http://adni.loni.usc.edu/wp-content/uploads/how_to_apply/ADNI_Acknowledgement_List.pdf).

**Funding** Beijing Natural Science Funds for Distinguished Young Scholars, China; Fundamental Research Funds for the Central Universities, China; National Natural Science Foundation, China.

**Copyright** © 2023 The Author(s). Published by Elsevier B.V. This is an open access article under the CC BY-NC-ND license (<http://creativecommons.org/licenses/by-nc-nd/4.0/>).

**Keywords:** Alzheimer's disease; Global signal; Transcriptomics; Functional network

### Research in context

#### Evidence before this study

The global signal (GS) is a traditional confounder that is removed from functional magnetic resonance imaging (fMRI) data. However, recent literature has shown the informative role of GS, suggesting that GS removal should be performed carefully based on a specific question. In addition to artifacts, GS represents an overall fluctuation of the global activity in the brain. Alzheimer's disease (AD) is a neurodegenerative disease associated with widespread disruptions in local specialization and global integration in the functional brain network. These changes in functional integration may further disrupt the spatial configuration of GS, which represents the local relative contribution to global brain activity. Investigations of GS can help guide GS removal and promote an understanding of alterations in the functional network in patients with AD.

#### Added value of this study

This study directly investigates the alterations in GS and its topography in patients with AD. The GS topography

shows a pattern of bidirectional changes in patients with AD compared with normal controls (NCs), suggesting that the spatial configuration of GS changed in individuals with AD. Meanwhile, topographic GS changes correlate with cognitive ability and brain functional network properties. Moreover, the genes identified based on GS topographical changes are enriched in pathways associated with AD and neurodegenerative diseases.

#### Implications of all the available evidence

These findings show a nonuniform pattern of alterations in local-global integration in the functional brain network of patients with AD, suggesting that cognitive impairment and functional network disruption might be linked to abnormal local-global integration. Additionally, the strong clinical relevance of GS topography indicates that global signal regression should be carefully performed in fMRI studies of patients with AD.

## Introduction

The global signal (GS) refers to the average signal of the gray matter voxels, representing an overall fluctuation of the global blood oxygen level-dependent (BOLD) activity. The GS is suggested to be linked to the artifacts of head motion, hardware, respiratory, and other unknown effects.<sup>1</sup> Therefore, it is regressed out as a nonneuronal signal in the preprocessing of fMRI data.<sup>2</sup> However, numerous studies have highlighted the potential biological mechanisms of GS,<sup>3–5</sup> providing convergent evidence that GS topography is related to human cognition and behavior.<sup>6,7</sup> The GS or its topography (i.e., the representation of GS in specific regions) was additionally reported to be associated with electrophysiological metrics,<sup>8</sup> tasks,<sup>9</sup> vigilance,<sup>10,11</sup> schizophrenia,<sup>12–15</sup> and autism spectrum disorder,<sup>16</sup> suggesting that GS may encompass neuronal signals in addition to nonneuronal signals. As a GS is composed of both neural and nonneuronal signals, a consensus has been established to determine whether to remove the GS based on the specific question.<sup>17</sup>

The human brain is organized into segregated complex systems with different functional areas that interact with each other for daily cognitive function.<sup>18,19</sup> Alzheimer's disease (AD) is a neurodegenerative disease associated with widespread disruptions in distinct

areas through disconnection mechanisms.<sup>20–22</sup> These widespread disruptions upset the balance between local specialization and global integration in the brain and consequently impair cognitive ability, affecting a patient's ability to perform daily tasks.<sup>23</sup> Several studies have documented that changes in global and local brain activity play important roles in advancing our understanding of AD.<sup>20,24,25</sup> Because substantial evidence has shown that the GS potentially reflects global neural activity, changes in the relationship between the global status and local activity might contribute to GS topographical changes.<sup>26</sup> Although the investigation of GS alterations is beneficial for guiding GS removal and understanding functional network disruptions, these changes have not been well studied in AD. Here, we proposed to investigate the contribution of GS topography in patients with AD to reveal the changes in the relationship between global integration and local specialization in individuals with AD, as well as to facilitate the preprocessing strategy for GS.

Because of the difficulties in eliminating artifacts from the GS, researchers should be careful when determining whether the alteration in the GS spatial configuration is due to neural changes or artifacts.<sup>1</sup> At the molecular level, single-cell activity is driven by

fluctuations in gene expression and protein synthesis in neurons.<sup>27,28</sup> Imaging transcriptomics has created a new opportunity to elucidate the molecular mechanism of brain function.<sup>29–31</sup> The utilization of transcriptional activity may reveal the potential biological basis of changes in the GS.

The primary purpose of this study was to explore the abnormal pattern of the GS and the potential biological mechanisms underlying this alteration. For this purpose, we utilized a large-sample fMRI dataset from the Multi-Center Alzheimer Disease Imaging Consortium Dataset (MCADI) as the discovery dataset. We first investigated the alterations in GS topography among patients with AD, participants with MCI, and normal controls (NCs). Then, we examined the relationship between alterations in GS topography and functional network organization (i.e., network integration and segregation). Next, the associations between GS topography and biological pathways were computed by performing spatial whole-brain gene mapping using the Allen Human Brain Atlas (AHBA).<sup>32,33</sup> Finally, we validated the robustness of our findings with samples from the Alzheimer's Disease Neuroimaging Initiative (ADNI).

## Methods

### Participants

The primary discovery dataset included 809 participants (including 257 NCs, 257 participants with MCI, and 295 patients with AD) from the MCADI.<sup>34–36</sup> All of the participants were enrolled in local hospitals in China. The discovery dataset was used to investigate the main findings of the study. Detailed information, including demographic, ethics, and clinical status, are presented in [Supplementary Methods S1](#) and [Table S1](#).

The validation dataset includes 542 subjects (265 NCs, 161 participants with MCI, and 116 patients with AD) from the ADNI (<http://adni.loni.usc.edu>) to replicate our analysis of the discovery dataset and verify the robustness of our findings. The detailed demographics and clinical information are shown in [Supplementary Methods S1](#) and [Table S1](#). Additional information about the ADNI dataset is available at [http://adni.loni.usc.edu/wp-content/uploads/how\\_to\\_apply/ADNI\\_Acknowledgement\\_List.pdf](http://adni.loni.usc.edu/wp-content/uploads/how_to_apply/ADNI_Acknowledgement_List.pdf).

### Image acquisition and preprocessing

The resting state (rs)-fMRI acquisition, preprocessing, and quality control were performed using the same protocols described in our previous studies.<sup>34,35</sup> Therefore, this section provides only a brief overview of these protocols, with further details provided in the [Supplemental material](#). All the rs-fMRI scans were preprocessed using the Brainnetome Toolkit (<http://brant.brainnetome.org>),<sup>37</sup> which included the following steps: (1) slice-timing correction; (2) realignment to the first volume; (3) spatial normalization to Montreal

Neurological Institute (MNI) space at 2 mm × 2 mm × 2 mm; (4) regression of nuisance signals, including linear trends, six motion parameters, and their first-order differences, and signals representing white matter and cerebrospinal fluid; (5) temporal bandpass filtering (0.01–0.08 Hz) to reduce high-frequency noise; and (6) Gaussian filtering with 6 mm full-width at half maximum (FWHM). Subsequently, any voxel where the mean absolute deviation in the fMRI signal was less than 0.05 was labeled absent; a voxel that was absent in more than 1% of individuals was excluded from the research.<sup>34</sup>

### Definition of the GS and GS topography

GS time series were obtained by averaging the signals of gray matter voxels, and the GS topography was estimated by calculating the GS correlation (GSCORR). For each voxel, the GSCORR was the Pearson correlation coefficient between the GS and its time series, which reflects the relative contribution of a voxel to the GS. The GSCORR was subsequently transformed by Fisher's *r*-to-*z* transformation to improve the normality of the correlation coefficients.

### The signal power of the GS

We estimated the signal power of the GS to determine the total alterations in BOLD activity in patients with AD. We computed the signal power in the frequency of the GS among the participants in the AD, MCI, and NC groups by performing a multitaper spectrum estimation with the Nitime Time-Series Analysis library (<http://nipy.org/nitime>). The mean signal power (across frequencies ranging from 0.01 to 0.08 Hz) of the GS showed failure in normality validation by Shapiro–Wilk test in the three groups separately or together ( $P_s < 0.05$ ) and therefore compared between participants in the AD, MCI, and NC groups using the Kruskal–Wallis test, which is a nonparametric method for testing whether samples originate from the same distribution. Considering the variation in different fMRI scanning lengths, we retained only the first 170 time points of fMRI data for each individual.

### Alteration of GS topography in patients with AD

A one-sample *t* test was applied to the GSCORR map for individuals to illustrate the spatial configuration of GS topography in each group. A general linear model (GLM) was then introduced to investigate the difference in GS topography between patients with AD and NCs while adjusting for age, sex, and site. The significant regions were identified by a voxel level threshold ( $P < 0.05$ , false discovery rate (FDR)-corrected) and a cluster threshold (cluster size  $>20$ ). Regions with significantly increased voxels and decreased voxels in the MCADI dataset were extracted separately as regions of interest (ROIs) for investigating the alterations in GSCORR. The average GSCORR for the increased ROIs

(iGSCORR) and the decreased ROIs (dGSCORR) were compared between participants with MCI and the other two groups using two-sample two-sided *t* tests to show the alterations in GSCORR in the early stage of AD. We performed correlation analyses of the iGSCORR and dGSCORR by calculating Spearman's coefficients between these values and the Mini-mental State Examination (MMSE) scores within each group after regressing out age, sex, and site effects to evaluate further whether the GSCORR in the significant areas changed within each clinical stage.

#### Alterations in network segregation and integration measurement in patients with AD

We performed a graph theory network analysis to investigate the potential contribution of the GS to functional network organization. An undirected functional network was constructed by measuring the functional correlations between 246 parcels according to the Brainnetome Atlas.<sup>38</sup> Node segregation in the functional network was primarily measured by calculating the clustering coefficients, which were determined as the ratio of the number of connections between the direct neighbors of the node to the total number of possible connections between these neighbors. Meanwhile, node integration in the brain was measured by determining the shortest path length, which is the average minimum number of connections that link any two nodes of the network.<sup>39</sup> The clustering coefficient and shortest path length were calculated with a range of sparsity thresholds (from 0.05 to 0.15, step of 0.01). Finally, a GLM was employed to compare the brain network segregation and integration between patients with AD and NCs while adjusting for age, sex, and site.

#### The association between changes in GSCORR and gene expression

The cortex and subcortex were parcellated into 246 parcels based on the Brainnetome Atlas.<sup>38</sup> We considered 123 brain parcels in the left hemisphere since the AHBA only includes data for the right hemisphere for two subjects.<sup>29</sup> The regional-based GSCORR was computed by averaging the GSCORR across all voxels included in this region, and region-based gene expression from AHBA was estimated using *abagen*.<sup>29,40</sup> Separate *z* score normalization procedures were applied for cortical and subcortical regions due to the strong anti-correlation between cortical and subcortical gene expression.<sup>41</sup> Regional changes in GSCORR (*t*-statistic) were assessed by performing a two-sample *t* test between patients with AD and NCs after controlling for age, sex, and data site.

Partial least squares (PLS) regression analysis between the changes in GS and gene expression was performed to identify the potential biological mechanism. PLS regression analysis has been widely used for transcriptomic analyses,<sup>42</sup> and it can find linear combinations of

weighted gene expression scores (predictor variables) that are the most predictive of GSCORR alterations (response variables).<sup>43</sup> We performed 1000 permutations using the surrogate maps generated from spin rotations in cortical regions and resampling of the subcortical regions to examine whether the explained variance in the component was significantly larger than that achieved by chance.<sup>44</sup> Then, the correlation between the PLS component and GS alterations was also examined using the same method to determine whether it was greater than chance. Furthermore, we performed bootstrapping to estimate the error of the weight of each gene, and the normalized weight of each gene was generated by dividing the weight by the estimated error.<sup>42</sup> Finally, we performed an enrichment analysis of Kyoto Encyclopedia of Genes and Genomes (KEGG) pathways for statistically significant genes using a background gene list of all human genes with "clusterprofiler" software.<sup>45</sup>

#### Replication analysis

The alterations in GSCORR between the participants in the AD and NC groups were compared again with the independent samples from the ADNI dataset to verify the robustness of the results. The protocol used for the analysis was the same as that described above. Then, correlation analyses between the MCADI and the ADNI database were performed for the GSCORR alterations to investigate whether the altered pattern was consistent between the two datasets. Spearman's correlation coefficient was calculated between the statistical map of the two datasets. Next, we mapped the results from MNI standard space to *fsaverage\_LR32k* and extracted voxels in subcortical areas (thalamus, basal ganglia, hippocampus, and cerebellum) to exclude the confounding effect driven by spatial autocorrelation. The spatial autocorrelation effect was excluded using the generative modeling implemented in BrainSMASH software to address the spatial autocorrelation effect of numerous subcortical voxels.<sup>46</sup> Furthermore, we investigated the GS topography using a GLM, which measured the contribution by calculating the beta coefficients (Supplementary Methods S3).<sup>13</sup> The correlation determined using Spearman's correlation analysis was also calculated between the GS beta map and the GSCORR map.

#### Role of the funding source

The funders supported the data collection but played no role in the study design, data analyses, interpretation, or writing of this manuscript.

## Results

### Alterations in the GS and GS topography in patients with AD

Participants from the MCADI were used in the discovery analysis to obtain results. No difference in the mean power of the GS was observed between the NC, MCI,

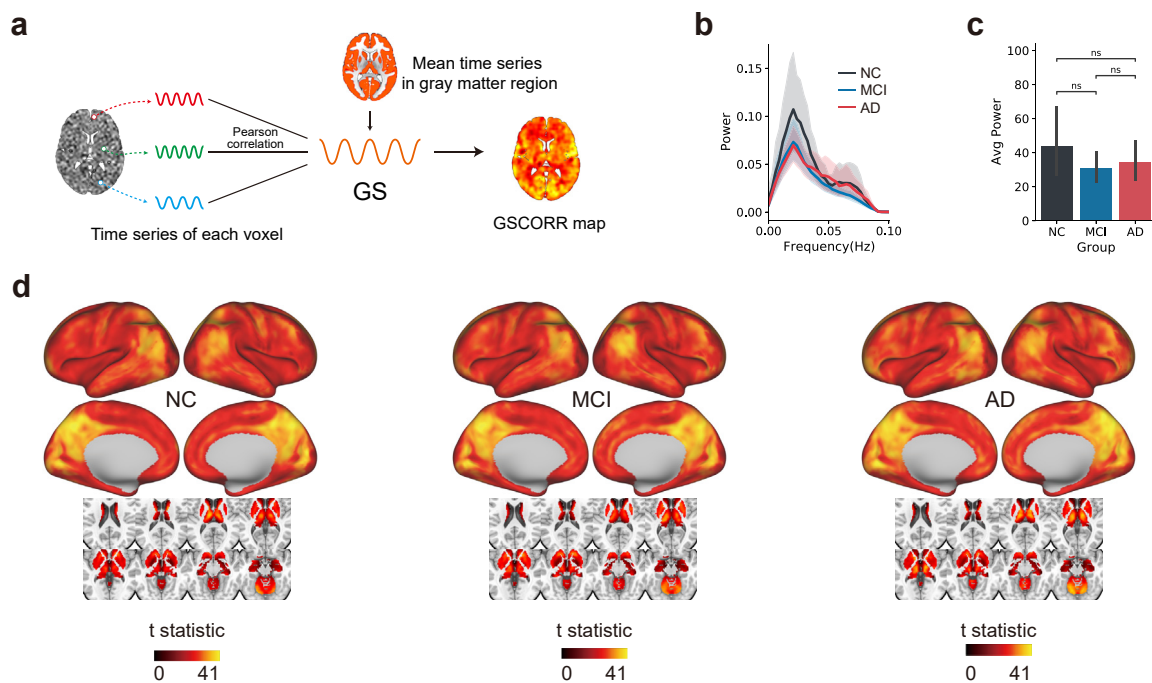


**Fig. 1: GS and GS spatial topography.** (a) An illustration of the calculation of GSCORR, which is a correlation between the GS and time series in each voxel. (b) The group-level average power of the GS in the NC, MCI, and AD groups in the frequency domain. (c) Comparisons of the average power of the GS across all frequencies among the three groups. (d) GSCORR topography (t-map of the one-sample t test) in the NC, MCI, and AD groups.

and AD groups ( $P = 0.41$ ), suggesting that the whole-brain activity showed no significant differences that were attributed to the disease (Fig. 1b and c).

In the analysis of GS topography, the results showed that participants in the NC, MCI, and AD groups had a similar GSCORR spatial pattern, which was higher in the posterior cingulate cortex/precuneus and inferior parietal lobule than in other regions (Fig. 1d). However, bidirectional alterations in GS topography were observed between patients with AD and NCs (Fig. 2a). Fig. 2b shows the significant regions that were compared between patients with AD and NCs ( $P < 0.05$ , FDR-corrected, and cluster size  $>20$ ). The GSCORR of participants in the AD group was increased in the middle frontal gyrus, inferior frontal gyrus, and thalamus and decreased in the cingulate gyrus, caudate, middle temporal gyrus, inferior parietal lobule, and hippocampus/parahippocampus (Supplementary Fig. S2).

We examined the relationship between head motion and the GS to evaluate whether head motion affected our results. The results showed no direct relationship between the clinical relevance of head motion and that of the GS in patients with AD (Supplementary Results S1). Furthermore, we applied the same method to the participants with strict criteria for head motion, which showed highly correlated patterns compared to those in the original dataset

(Supplementary Results S2, Fig. S3), indicating that the effect of head motion was small.

The regions that constituted significantly increased voxels and decreased voxels were extracted separately as ROIs based on the GSCORR alterations in the MCADI dataset (Supplementary Fig. S2). In the MCADI dataset, participants with MCI showed a higher level of dGSCORR than participants with AD ( $t = 4.90$ ,  $P = 1.25e-6$ ) and a lower dGSCORR than NCs ( $t = -3.77$ ,  $P = 1.98e-4$ ) (Fig. 2c). Interestingly, the dGSCORR significantly correlated with the MMSE score of patients with AD (Spearman's coefficient  $\rho = 0.13$ ,  $P = 0.024$ ) and had no significant relationships in NCs ( $P = 0.88$ ) and participants with MCI ( $P = 0.078$ ) (Fig. 2d). Participants with MCI showed a lower iGSCORR than those with AD ( $t = -4.55$ ,  $P = 6.23e-6$ ) and a higher GSCORR than NCs ( $t = 3.14$ ,  $P = 1.80e-3$ ) (Fig. 2e). The iGSCORR was also significantly correlated with the MMSE score of patients with AD ( $\rho = -0.13$ ,  $P = 0.030$ ) and showed no significant correlation with the MMSE score of NCs ( $P = 0.81$ ) and participants with MCI ( $P = 0.21$ ) (Fig. 2f).

We further analyzed the samples from the ADNI using the same ROIs to validate the finding of cognitive relevance and alteration of dGSCORR and iGSCORR. Similar alteration patterns and cognitive associations were observed in the groups by analysis of variance (Fig. 2g–j), showing the authenticity of the cognitive

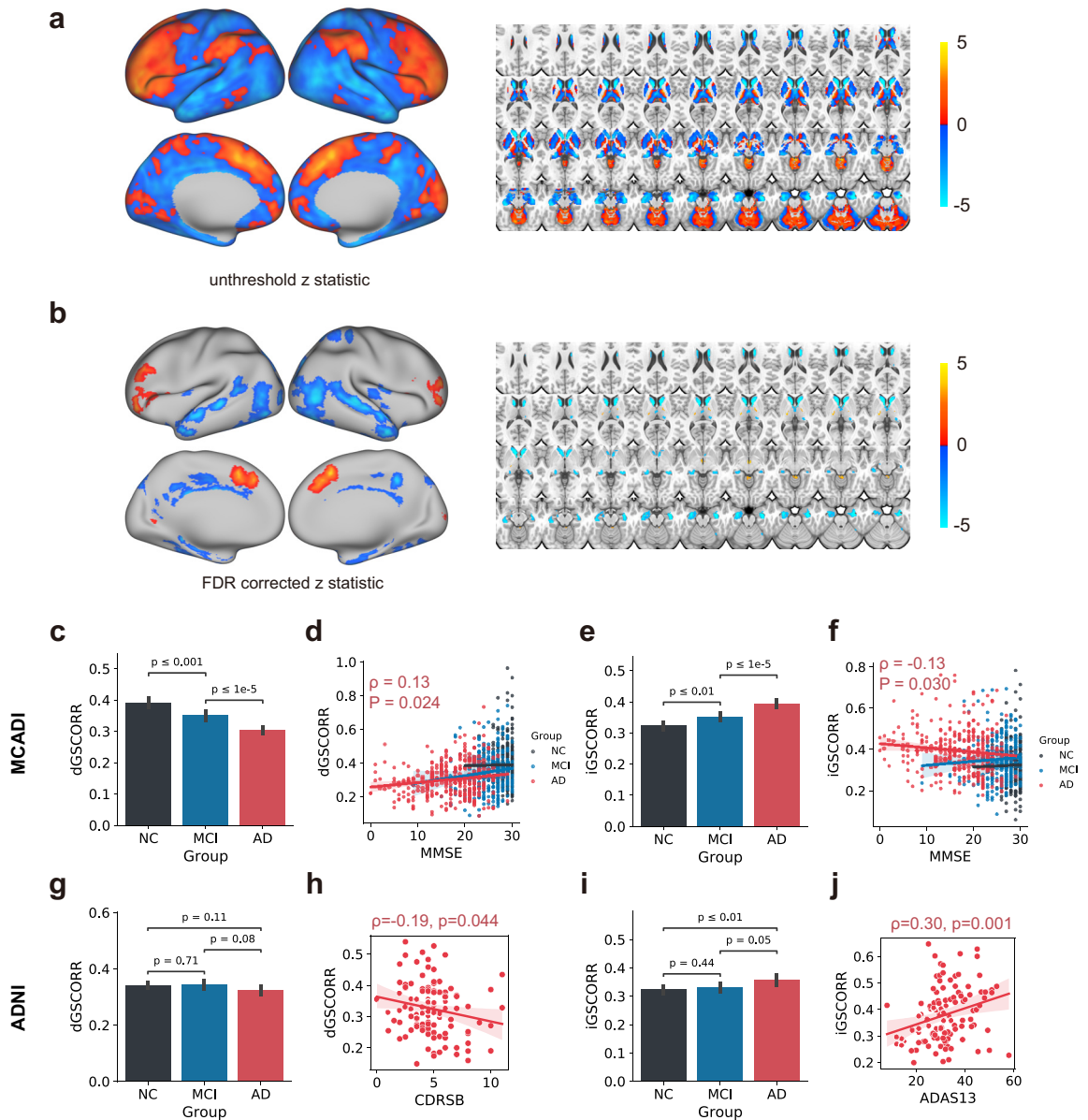


**Fig. 2: Altered GSCORR in patients with AD.** (a) Unthresholded z-map of the comparison between individuals with AD and NCs. (b) Areas showing significant differences between patients with AD and NCs (FDR-corrected  $P < 0.05$  and cluster size  $>20$ ). (c) Comparison of the average GSCORR in the decreased area (dGSCORR) between the MCI group and the other two groups in MCADI. (d) Scatterplot of the relationship between MMSE scores and dGSCORR scores of participants within each group in MCADI. The labeled figure indicates the correlation within the AD group. (e) Comparison of the average GSCORR in the increased area (iGSCORR) between the MCI group and the other two groups in MCADI. (f) Scatterplot of the relationship between MMSE scores and iGSCORR scores of participants within each group in MCADI. The labeled figure indicates the correlation within the AD group. (g) Comparison of the dGSCORR among participants in the NC, MCI, and AD groups in ADNI. (h) Scatterplot of the relationship between cognition (CDRSB scores) and dGSCORR scores of participants in the AD groups in ADNI. (i) Comparison of the iGSCORR among participants in the NC, MCI, and AD groups in ADNI. (j) Scatterplot of the relationship between cognition (ADAS13 scores) and iGSCORR scores of participants in the AD groups in ADNI.

relevance. The dGSCORR did not show a significant difference among participants in the NC, MCI, and AD groups ( $F = 1.69$ ,  $P = 0.180$ ) after regressing the effects of age and sex (Fig. 2g). However, the dGSCORR was

still significantly correlated with the CDRSB in patients with AD ( $\rho = -0.19$ ,  $P = 0.044$ ) (Fig. 2h). The iGSCORR also showed a significant difference among participants in the NC, MCI, and AD groups ( $F = 4.23$ ,  $P = 0.023$ )

after regressing the effects of age and sex (Fig. 2i). Participants with AD showed a higher iGSCORR than NCs ( $t = 2.85$ ,  $P = 0.005$ ) and a similar level to participants with MCI ( $t = 1.93$ ,  $P = 0.054$ ). The iGSCORR was also significantly correlated with ADAS13 in patients with AD (Spearman's correlation coefficient  $\rho = 0.30$ ,  $P = 0.001$ ) (Fig. 2j).

### Relationship between changes in GSCORR and network organization

The regional changes in GSCORR strongly corresponded to the voxel-level results in the MCADI dataset (Fig. 3a). Interestingly, the changes in network organization showed a strong relationship with the changes in GSCORR. At the sparse threshold of 0.08, the increased chances of a clustering coefficient and decreased chances of the shortest path length located in the frontal lobe and inferior parietal lobule were similar to the changes in GSCORR (Spearman's coefficient  $\rho = 0.50$  and  $\rho = -0.57$ , respectively) (Fig. 3b and c, results for other thresholds are shown in Supplementary Fig. S2).

### Mapping changes in GS topography to gene expression

Associations between GS topography and gene expression were determined in the MCADI dataset. PLS identified a gene expression profile with high expression in the frontal and parietal cortices. The first component of the PLS (PLS1, explained variance = 0.38,  $P_{perm} = 0.004$ ) was the linear combination of gene expression levels that were most strongly correlated with regional changes in GSCORR ( $\rho = 0.60$ ,  $P_{perm} < 0.001$ ) (Fig. 4a and b). The subset of 3772 positively and negatively weighted genes ( $|z| > 3$ ) comprised a topologically interactive network that was enriched for

several KEGG pathways (Fig. 4d and Fig. S5).<sup>42</sup> The identified KEGG pathways have been reported to modulate a wide variety of neurodegenerative diseases, including AD, Huntington's disease, amyotrophic lateral sclerosis, prion disease, and Parkinson's disease. Apart from these diseases, the genes identified by PLS1 were also enriched in pathways associated with thermogenesis, chemical carcinogenesis-reactive oxygen species, autophagy, and oxidative phosphorylation, among others. Enrichment analysis was also performed when choosing the 1964 genes identified with another threshold ( $|z| > 4$ ), and a consistent result was obtained (Supplementary Fig. S5).

### Replication analysis

With the replication samples from ADNI, the GSCORR of each group (i.e., NC, MCI, and AD) in the ADNI dataset showed a similar spatial pattern compared to that in the MCADI dataset, which was mainly located in the posterior cortex, including the visual cortex and parietal lobe (Fig. 5). The changes observed in patients with AD compared with NCs were mainly an increased GSCORR in the superior frontal lobe and inferior parietal lobule and decreased GSCORR in the posterior superior temporal sulcus (Fig. 5g). All the results were significantly correlated in the spatial distribution between the two datasets at the surface level after controlling for the spatial autocorrelation effect (all  $P$  values  $< 0.001$ , Fig. 5b, d, f, h). The significant association was consistent when correlating the values at the volume level without controlling for the spatial autocorrelation effect (Fig. S6). Furthermore, highly similar patterns of GS topography were also observed in the GS beta map ( $\rho = 0.74$ ,  $P < 0.001$ , Fig. S7).

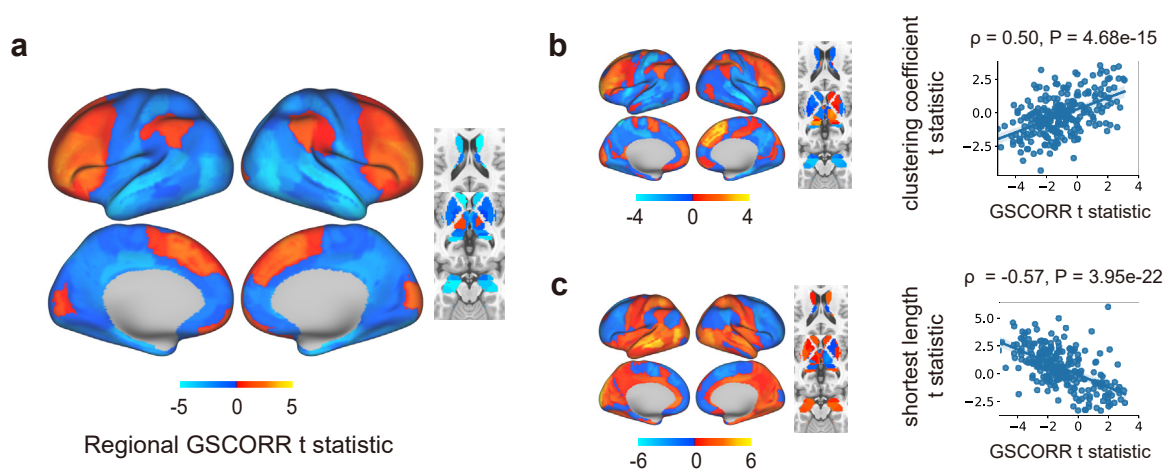


**Fig. 3: Relationship with network organization.** (a) T-map of regional GSCORR for the comparison between participants in the AD and NC groups. (b) Scatterplot of regional t-statistic values of GSCORR vs. regional t-statistic values of the clustering coefficient (sparse threshold = 0.08). (c) Scatterplot of regional t-statistic values of GSCORR vs. regional t-statistic values of the shortest path length (sparse threshold = 0.08).

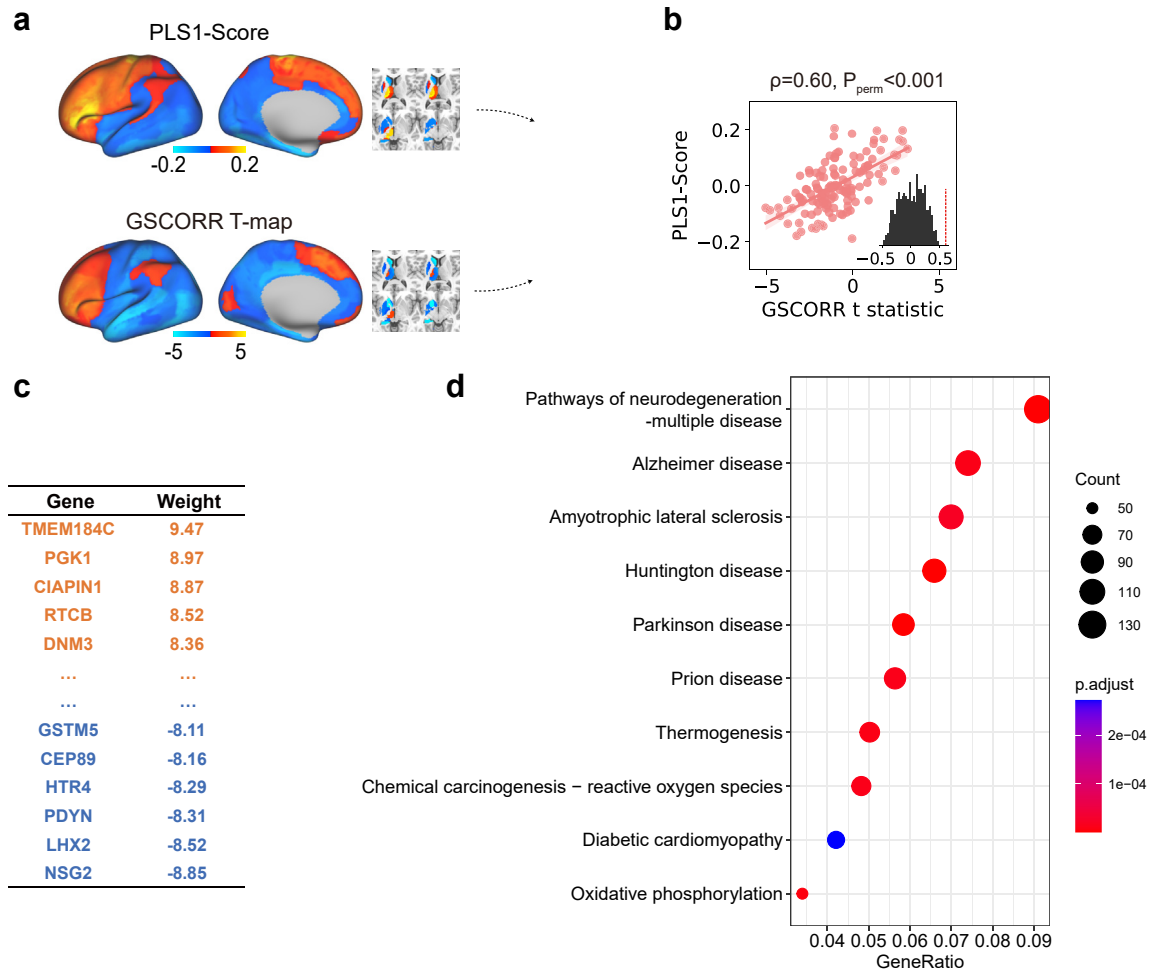


**Fig. 4: Mapping the changes in GSCORR topology to gene expression.** (a) Regional (left side of Brainnetome Atlas) PLS1 scores of genes and regional GSCORR alterations in the MCADI dataset. (b) Scatterplot of PLS1 scores vs. regional t-statistic (AD vs. NCs) of the regional GSCORR alteration. (c) Genes that positively and negatively weighted PLS1 values for the subsequent KEGG pathway enrichment. (d) KEGG terms for PLS1 genes. The size of the circle represents the number of genes involved in the specific term, and the color represents the corrected P values ( $P < 0.05$ , FDR-corrected).

### Discussion

In the present study, we initially investigated alterations in the GS in patients with AD, which is essential for understanding the changes in global functional activity in patients with AD. Our results provided convergent evidence that the GS topography exhibited a pattern of bidirectional changes in patients with AD, which was strongly related to network segregation and integration. Moreover, alterations in GS topography were associated with the genetic foundation of AD and multiple neurodegenerative diseases. Furthermore, the reproducibility of GS alterations between the MCADI and ADNI datasets, which include large samples from multiple centers and are representative of the AD populations with different ethnicities from China and North America, confirmed the generalization of the clinical relevance of

the GS in patients with AD. The spatial reconfiguration, clinical relevance, association with the functional network, and potential molecular associations with diseases of the GS might contribute to studies of the functional system in individuals with AD in the future.

Although the GS is suggested to be linked to artifacts, which usually should be regressed out when preprocessing fMRI data, several studies have found that GS topography is potentially modulated by neuronal factors.<sup>3,4</sup> The nonuniform modulation of the GS, which might be associated with functional changes in various regions,<sup>9</sup> was detected in patients with AD by investigating the GSCORR. The GS topography observed in the present study reflects the high GSCORR located in the posterior cortex of the brain in NCs, similar to previous studies.<sup>9,13</sup> Several studies consistently found

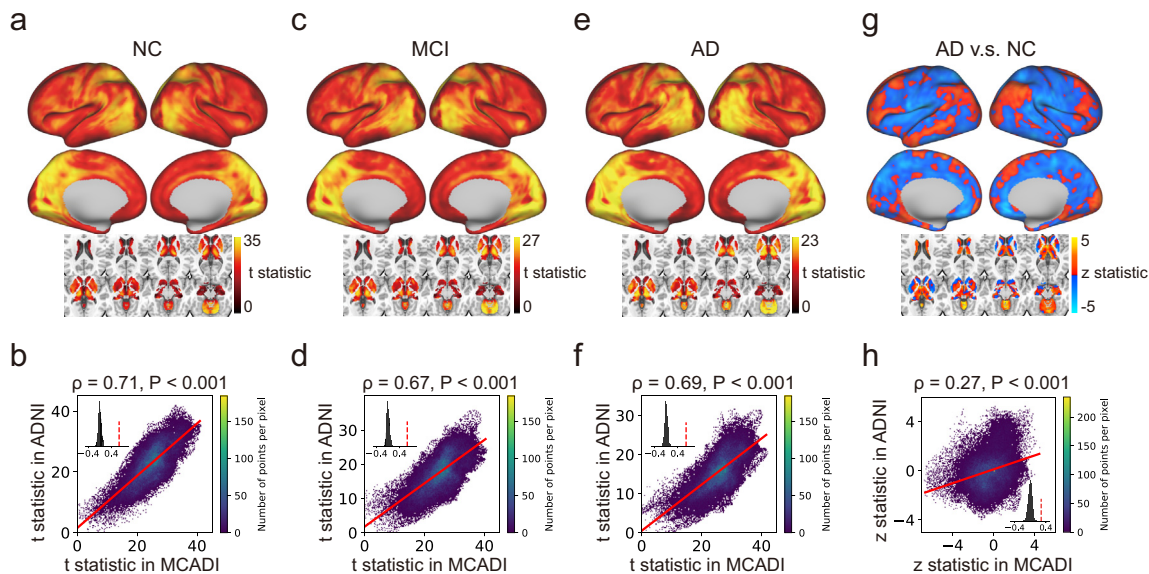


**Fig. 5: Replication analysis of GSCORR using ADNI data.** (a–b) Replication of GSCORR for participants in the NC group. The top panel shows the T-map of the NCs in the ADNI dataset, and the bottom scatterplot shows the significant correlation between the two datasets. (c–d) Replication of GSCORR in participants with MCI. The top panel shows the T-map of the MCI in the ADNI, and the bottom scatterplot shows the significant correlation between the two datasets. (e–f) Replication of GSCORR in patients with AD. The top panel shows the T-map of patients with AD in the ADNI dataset, and the bottom scatterplot shows the significant correlation between the two datasets. (g–h) Replication of the differences in GSCORR between participants in the AD and NC groups. The top panel shows the z-map of the comparison between participants in the AD and NC groups in the ADNI dataset, and the bottom scatterplot shows the significant correlation between the two datasets. (The histogram inside the scatterplot shows the null model derived from the spatial autocorrelation surrogates.)

that functional activity within the frontal lobe is increasingly altered with the development of AD,<sup>23,47–50</sup> and the frontal lobe was proposed to be a substrate of functional compensation to resist cognitive disability.<sup>51,52</sup> Compared with NCs, the GSCORR in patients with AD was also elevated in the middle frontal gyrus, suggesting that the increased functional activity in the frontal lobe increased its relative contributions to global neuronal activity. Our results showed that GSCORR values in patients were decreased in several hub regions of the default mode network, including the cingulate gyrus, precuneus, middle temporal gyrus, and hippocampus/parahippocampus, compared with those of NCs. The default mode network is preferentially disrupted in patients with AD and is associated not only with various cognitive functions and episodic memory but also with amyloid deposits.<sup>21,53</sup> Another notable area is the caudate, which is impaired in patients with AD but has received less attention than the hippocampus.<sup>54–56</sup> The caudate plays an important role in learning, and the stimulation of this region may modulate learning-related changes in the power of the dorsolateral prefrontal cortex.<sup>57</sup> The GSCORR in the bilateral caudate exhibited a clustered alteration, suggesting that the synchronization between caudate and global neuronal activity changed extensively.

Furthermore, the changes in GSCORR were strongly correlated with functional network organization and cognition. This finding is supported by previous studies showing that the integration and segregation of functional networks changed and played an essential role in the progression of AD.<sup>20,23–25</sup> Based on our results, global-local coupling was indeed changed and driven by the disease and might be a factor underlying network segregation. The average GSCORR was significantly correlated with cognitive ability in patients with AD, indicating that GS alterations are associated with underlying pathological changes. Moreover, the altered GSCORR showed a progressive trend among the three groups in several important functional systems, which provides further evidence that GS alterations might provide an opportunity to track disease progression.

AD is extensively associated with motor dysfunction,<sup>58</sup> and individuals with AD tend to exhibit more head motion than normal individuals.<sup>59</sup> Motor dysfunction may cause more unconscious motions, and the artifacts derived from head motion were identified in previous studies<sup>60,61</sup>; therefore, studies using fMRI usually regressed out the head motion and controlled the head motion of subjects by thresholding the values of FD.<sup>62</sup> Interestingly, no difference in the sum of FD was observed between participants in the AD and NC

groups, significant differences in the signal power of FD were still detected. Meanwhile, the signal power of head motion in patients with AD is higher than that in NCs, but the power of the GS in NCs is comparable to that in patients with AD, suggesting that the signal driven by head motion did not dominate the GS. We further investigated the head motion correlation (framewise displacement correlation, FDCORR), which showed a high representation in the sensorimotor cortex (Fig. S9). This representation partially revealed that those conscious or unconscious tiny movements had a tight relationship with the functional activities in the sensorimotor cortex. Hence, the relatively low GSCORR in the sensorimotor cortex compared with previous studies may be due to the use of different head motion criteria.

Moreover, AD has a vital genetic component,<sup>63</sup> which helps us to prove that the alteration in GS topography is attributed to the disease. Previous studies have confirmed that GSs show different alterations in individuals with different psychiatric disorders (i.e., schizophrenia and bipolar disorder<sup>14</sup>) or different phases of psychiatric disorders (i.e., manic, depressive, and euthymic of bipolar disorder<sup>26</sup>). According to the genetic association with AD, our results further confirmed that patients with AD had a different pattern of GS alterations than patients with psychiatric disorders. Moreover, the genes are enriched not only in the AD-associated pathway but also in multiple neurodegenerative disease pathways, reflecting a potential mechanism shared by a series of neurodegenerative diseases. The basal ganglia might be a bridge that connects GS alterations in individuals with AD with those of patients with other diseases. For example, the major pathological site of Huntington's disease is located in the basal ganglia, particularly the caudate,<sup>64</sup> and Parkinson's disease also had structural alteration in the basal ganglia and medial temporal lobe.<sup>65</sup> AD and amyotrophic lateral sclerosis have an etiopathogenic connection linked to inhibitor-2 of protein phosphatase-2A.<sup>66</sup> Prion disease and AD have different neuropathologies, but both are strongly associated with neuroinflammation,<sup>67,68</sup> and prion disease may even trigger biochemical changes similar to those triggered by AD.<sup>69</sup> In addition to related neurodegenerative diseases, other pathways, such as autophagy, also showed strong associations with AD.<sup>70</sup> Mitochondrial defects are known to occur in aging, cancer, heart disease, and a wide variety of degenerative diseases,<sup>71</sup> and increasing evidence implicates mitochondrial dysfunction resulting from molecular defects in oxidative phosphorylation.<sup>71</sup> A $\beta$  and tau synergistically impair the oxidative phosphorylation system.<sup>72</sup> A superficial relationship between diabetic cardiomyopathy and AD was not observed, but underlying correlations existed beneath the surface. Diabetes is a typical metabolic disease that is closely correlated with abnormal thermogenesis,<sup>73</sup> and impaired thermoregulation is associated with AD-like neuropathology.<sup>74</sup> In conclusion, the

enriched pathways derived from PLS1 of GSCORR collectively suggested the neuropathogenesis underlying AD and related neurodegenerative diseases, which not only strongly suggested the informative role of GS but also revealed the associated molecular mechanisms of the altered GS topography.

More importantly, our findings provide instructive information about the global signal regression, which should be performed depending on the specific topic.<sup>17</sup> The GSR usually results in some difference in the analysis of fMRI data, and it is important to examine the relationship between GSR and disease-related changes.<sup>26,75</sup> Brain global connectivity is powerful for measuring connectivity of the brain network and has been shown to correlate with GS spatial patterns.<sup>26,76</sup> We also investigated the effect of GSR on alterations in the global connectivity of the brain in patients with AD (Supplementary Results S3). The increased area of global connectivity in the brain was expanded in the comparison between AD and NC groups with GSR compared with that without GSR. The changes might be attributed to the attenuation of nonneural artifacts and be a more accurate result.<sup>14,17</sup> However, the alteration in the GS was not directly driven by head motion and correlated with cognition, brain network properties, and the molecular mechanism of AD, suggesting that alterations are driven by the disease. Hence, our findings indicated that GSR should be performed carefully in studies of patients with AD, and reporting both results will be beneficial for interpreting disease-related changes.<sup>14,75</sup>

This study had several limitations. First, insufficient physiological and pathological data may have restricted the current findings. The GS was suggested to be closely associated with physiological noise and motion.<sup>1</sup> The effect of head motion was minimized to prevent noise and confirmed to have a limited effect on the between-group comparisons. We further validated the main results when removing the individuals with correlations between GS and FD. Future studies would enrich our findings by analyzing neurobiological data (i.e., imaging data of A $\beta$  and tau) to further verify the pathological basis of GS alterations. Second, other neuroimaging modalities might be complementary in understanding the alterations in the GS in patients with AD. Specifically, anatomical connectivity derived from diffusion MRI would be one of our focuses in future studies to identify the relationship between areas with an altered GS. Third, patients who had comorbidities with other disorders were excluded. The brains of elderly individuals usually are affected by multiple proteinopathies and vascular injuries.<sup>77</sup> Investigating the effects of comorbidities on AD is also important for assessing neuropathology and clinical phenotypes in individuals with dementia. Cohorts containing participants with multiple diseases and comorbidity information are promising for a large contribution to AD and AD-

associated dementia research in the future. Finally, the regional gene expression patterns identified in the six postmortem brains from the AHBA dataset represent a conserved canonical signature of healthy subjects.<sup>78</sup> Although imaging transcriptomics contributed to the understanding of the macroscopic neuroimaging phenotypes, the association is a potential interpretation and not a direct molecular basis. A promising approach is to investigate the molecular mechanism of GS by combining gene expression data from participants with AD and genome-wide association studies when the relevant data are available.

In summary, the present study initially characterized AD dementia-associated changes in the GS using two large AD rs-fMRI databases, and the relevant findings were quite robust, based on the validation analysis. GS topography displayed a pattern of bidirectional changes in patients with AD, and alterations in GS topography were associated with the brain network organization and pathways of AD and multiple neurodegenerative diseases. These findings highlight the relationship between local and global neuronal activity that is changed during disease progression and provide a new perspective for understanding the disruption of brain functions in patients with AD.

#### Contributors

Wrote the draft: Pindong Chen and Kun Zhao; Study design: Pindong Chen, Yong Liu, Yongbin Wei, and Tianzi Jiang; Data collection: Pan Wang, Dawei Wang, Chengyuan Song, Hongwei Yang, Zengqiang Zhang, Hongxiang Yao, Tong Han, Chunshui Yu, Bo Zhou, Yuying Zhou, Jie Lu, Ying Han, and Xi Zhang; Data processing: Pindong Chen; Statistical analysis: Pindong Chen and Yong Liu; Manuscript revision: Kun Zhao, Han Zhang, Yongbin Wei, Yong Liu, Yida Qu, Xiaopeng Kang, Kai Du, Lingzhong Fan, and Bing Liu; Data access and verification: Pindong Chen, Kun Zhao, and Yong Liu. All authors read and approved the final version of the manuscript.

#### Data sharing statement

The data that support the findings of this study are available from the corresponding author upon reasonable request. All ADNI data are deposited in a publicly accessible repository and can be accessed at [adni.loni.usc.edu](https://adni.loni.usc.edu). The code that was used can be obtained at GitHub (<https://github.com/YongLiuLab>).

#### Declaration of interests

PW reports grants from the National Natural Science Foundation of China, during the conduct of the study; DW reports grants from the National Natural Science Foundation of China, during the conduct of the study; YH reports grants from the National Natural Science Foundation of China, during the conduct of the study; XZ reports grants from National Natural Science Foundation of China, during the conduct of the study; YL reports grants from Ministry of Education of the People's Republic of China, grants from Beijing Natural Science Funds, grants from National Natural Science Foundation of China, during the conduct of the study. The remaining authors reported no relevant conflicts.

#### Acknowledgments

Data collection and sharing for this project were funded by the Alzheimer's Disease Neuroimaging Initiative (ADNI) (National Institutes of Health Grant U01 AG024904) and DOD ADNI (Department of Defense award number W81XWH-12-2-0012). ADNI is funded by the National Institute on Aging, the National Institute of Biomedical Imaging and Bioengineering, and through generous contributions from the following

companies: AbbVie, Alzheimer's Association; Alzheimer's Drug Discovery Foundation; Araclon Biotech; BioClinica, Inc.; Biogen; Bristol-Myers Squibb Company; CereSpir, Inc.; Cogstate; Eisai Inc.; Elan Pharmaceuticals, Inc.; Eli Lilly and Company; EuroImmun; F. Hoffmann-La Roche Ltd. and its affiliated company Genentech, Inc.; Fujirebio; GE Healthcare; IXICO; Janssen Alzheimer Immunotherapy Research & Development, LLC.; Johnson & Johnson Pharmaceutical Research & Development LLC.; Lumosity; Lundbeck; Merck & Co., Inc.; Meso Scale Diagnostics, LLC.; NeuroRx Research; Neurotrack Technologies; Novartis Pharmaceuticals Corporation; Pfizer Inc.; Piramal Imaging; Servier; Takeda Pharmaceutical Company; and Transition Therapeutics. The Canadian Institutes of Health Research provides funds to support ADNI clinical sites in Canada. Private sector contributions are facilitated by the Foundation for the National Institutes of Health ([www.fnih.org](http://www.fnih.org)). The grantee organization is the Northern California Institute for Research and Education, and the study was coordinated by the Alzheimer's Therapeutic Research Institute at the University of Southern California. ADNI data are disseminated by the Laboratory for Neuro Imaging at the University of Southern California.

This work was partially supported by grants from the Beijing Natural Science Funds for Distinguished Young Scholars (No. JQ20036), the Fundamental Research Funds for the Central Universities (No. 2021XD-A03), and the National Natural Science Foundation of China (Nos. 81871438, 82172018, and 81901101). Data collection and sharing for this project were funded by the National Natural Science Foundation of China (Grant Nos. 61633018, 81571062, 81400890, and 81471120).

#### Appendix A. Supplementary data

Supplementary data related to this article can be found at <https://doi.org/10.1016/j.ebiom.2023.104455>.

#### References

- Power JD, Plitt M, Laumann TO, Martin A. Sources and implications of whole-brain fMRI signals in humans. *Neuroimage*. 2017;146:609–625.
- Aquino KM, Fulcher BD, Parkes L, Sabarodien K, Fornito A. Identifying and removing widespread signal deflections from fMRI data: rethinking the global signal regression problem. *Neuroimage*. 2020;212:116614.
- Liu X, de Zwart JA, Scholvinck ML, et al. Subcortical evidence for a contribution of arousal to fMRI studies of brain activity. *Nat Commun*. 2018;9(1):395.
- van den Heuvel MP, Kahn RS, Goni J, Sporns O. High-cost, high-capacity backbone for global brain communication. *Proc Natl Acad Sci U S A*. 2012;109(28):11372–11377.
- Gotts SJ, Gilmore AW, Martin A. Brain networks, dimensionality, and global signal averaging in resting-state fMRI: hierarchical network structure results in low-dimensional spatiotemporal dynamics. *Neuroimage*. 2020;205:116289.
- Chen X, Liao X, Dai Z, et al. Topological analyses of functional connectomics: a crucial role of global signal removal, brain parcellation, and null models. *Hum Brain Mapp*. 2018;39(11):4545–4564.
- Fox MD, Zhang D, Snyder AZ, Raichle ME. The global signal and observed anticorrelated resting state brain networks. *J Neurophysiol*. 2009;101(6):3270–3283.
- Scholvinck ML, Maier A, Ye FQ, Duyn JH, Leopold DA. Neural basis of global resting-state fMRI activity. *Proc Natl Acad Sci U S A*. 2010;107(22):10238–10243.
- Zhang J, Huang Z, Tumati S, Northoff G. Rest-task modulation of fMRI-derived global signal topography is mediated by transient coactivation patterns. *PLoS Biol*. 2020;18(7):e3000733.
- Wong CW, DeYoung PN, Liu TT. Differences in the resting-state fMRI global signal amplitude between the eyes open and eyes closed states are related to changes in EEG vigilance. *Neuroimage*. 2016;124:24–31.
- Wong CW, Olafsson V, Tal O, Liu TT. The amplitude of the resting-state fMRI global signal is related to EEG vigilance measures. *Neuroimage*. 2013;83:983–990.
- Hahamy A, Calhoun V, Pearlson G, et al. Save the global: global signal connectivity as a tool for studying clinical populations with functional magnetic resonance imaging. *Brain Connect*. 2014;4(6):395–403.

- 13 Yang GJ, Murray JD, Glasser M, et al. Altered global signal topography in schizophrenia. *Cereb Cortex*. 2017;27(11):5156–5169.
- 14 Yang GJ, Murray JD, Repovs G, et al. Altered global brain signal in schizophrenia. *Proc Natl Acad Sci U S A*. 2014;111(20):7438–7443.
- 15 Wang X, Liao W, Han S, et al. Altered dynamic global signal topography in antipsychotic-naïve adolescents with early-onset schizophrenia. *Schizophr Res*. 2019;208:308–316.
- 16 Gotts SJ, Saad ZS, Jo HJ, Wallace GL, Cox RW, Martin A. The perils of global signal regression for group comparisons: a case study of Autism Spectrum Disorders. *Front Hum Neurosci*. 2013;7:356.
- 17 Murphy K, Fox MD. Towards a consensus regarding global signal regression for resting state functional connectivity MRI. *Neuroimage*. 2017;154:169–173.
- 18 Power JD, Cohen AL, Nelson SM, et al. Functional network organization of the human brain. *Neuron*. 2011;72(4):665–678.
- 19 Sporns O. *Networks of the Brain*. MIT press; 2010.
- 20 Dai Z, He Y. Disrupted structural and functional brain connectomes in mild cognitive impairment and Alzheimer's disease. *Neurosci Bull*. 2014;30(2):217–232.
- 21 Dennis EL, Thompson PM. Functional brain connectivity using fMRI in aging and Alzheimer's disease. *Neuropsychol Rev*. 2014;24(1):49–62.
- 22 Wang JH, Zuo XN, Dai ZJ, et al. Disrupted functional brain connectome in individuals at risk for Alzheimer's disease. *Biol Psychiatr*. 2013;73(5):472–481.
- 23 Liu Y, Yu C, Zhang X, et al. Impaired long distance functional connectivity and weighted network architecture in Alzheimer's disease. *Cereb Cortex*. 2014;24(6):1422–1435.
- 24 Ewers M, Luan Y, Frontzkowski L, et al. Segregation of functional networks is associated with cognitive resilience in Alzheimer's disease. *Brain*. 2021;144(7):2176–2185.
- 25 Wang R, Liu M, Cheng X, Wu Y, Hildebrandt A, Zhou C. Segregation, integration, and balance of large-scale resting brain networks configure different cognitive abilities. *Proc Natl Acad Sci U S A*. 2021;118(23).
- 26 Zhang J, Magioncalda P, Huang Z, et al. Altered global signal topography and its different regional localization in motor cortex and Hippocampus in mania and depression. *Schizophr Bull*. 2019;45(4):902–910.
- 27 Tripathy SJ, Toker L, Li B, et al. Transcriptomic correlates of neuron electrophysiological diversity. *PLoS Comput Biol*. 2017;13(10):e1005814.
- 28 Cadwell CR, Palasantza A, Jiang XL, et al. Electrophysiological, transcriptomic and morphologic profiling of single neurons using Patch-seq. *Nat Biotechnol*. 2016;34(2):199–203.
- 29 Arnatkeviciute A, Fulcher BD, Fornito A. A practical guide to linking brain-wide gene expression and neuroimaging data. *Neuroimage*. 2019;189:353–367.
- 30 Richiardi J, Altmann A, Milazzo AC, et al. BRAIN NETWORKS. Correlated gene expression supports synchronous activity in brain networks. *Science*. 2015;348(6240):1241–1244.
- 31 Fulcher BD, Fornito A. A transcriptional signature of hub connectivity in the mouse connectome. *Proc Natl Acad Sci U S A*. 2016;113(5):1435–1440.
- 32 Sunkin SM, Ng L, Lau C, et al. Allen Brain Atlas: an integrated spatio-temporal portal for exploring the central nervous system. *Nucleic Acids Res*. 2013;41(Database issue):D996–D1008.
- 33 Hawrylycz MJ, Lein ES, Guillozet-Bongaarts AL, et al. An anatomically comprehensive atlas of the adult human brain transcriptome. *Nature*. 2012;489(7416):391–399.
- 34 Jin D, Wang P, Zalesky A, et al. Grab-AD: generalizability and reproducibility of altered brain activity and diagnostic classification in Alzheimer's Disease. *Hum Brain Mapp*. 2020;41(12):3379–3391.
- 35 Li J, Jin D, Li A, et al. ASAF: altered spontaneous activity fingerprinting in Alzheimer's disease based on multisite fMRI. *Sci Bull*. 2019;64(14):998–1010.
- 36 Chen P, Yao H, Tijms BM, et al. Four distinct subtypes of Alzheimer's disease based on resting-state connectivity biomarkers. *Biol Psychiatr*. 2022. <https://doi.org/10.1016/j.biopsych.2022.06.019>.
- 37 Xu K, Liu Y, Zhan Y, Ren J, Jiang T. BRANT: a versatile and extendable resting-state fMRI Toolkit. *Front Neuroinf*. 2018;12:52.
- 38 Fan L, Li H, Zhuo J, et al. The human brainnetome atlas: a new brain atlas based on connectonal architecture. *Cereb Cortex*. 2016;26(8):3508–3526.
- 39 Rubinov M, Sporns O. Complex network measures of brain connectivity: uses and interpretations. *Neuroimage*. 2010;52(3):1059–1069.
- 40 Markello R, Shafiei G, Zheng Y-Q, Mišić B. *abagen: A toolbox for the Allen Brain Atlas genetics data*. Zenodo; 2021.
- 41 Hawrylycz M, Miller JA, Menon V, et al. Canonical genetic signatures of the adult human brain. *Nat Neurosci*. 2015;18(12):1832–1844.
- 42 Morgan SE, Seidlitz J, Whitaker KJ, et al. Cortical patterning of abnormal morphometric similarity in psychosis is associated with brain expression of schizophrenia-related genes. *Proc Natl Acad Sci U S A*. 2019;116(19):9604–9609.
- 43 Li L, Wei Y, Zhang J, et al. Gene expression associated with individual variability in intrinsic functional connectivity. *Neuroimage*. 2021;245:118743.
- 44 Giacomel A, Martins D, Frigo M, et al. Integrating neuroimaging and gene expression data using the imaging transcriptomics toolbox. *STAR Protoc*. 2022;3(2):101315.
- 45 Yu GC, Wang LG, Han YY, He QY. clusterProfiler: an R Package for comparing biological themes among gene clusters. *OMICS*. 2012;16(5):284–287.
- 46 Burt JB, Helmer M, Shinn M, Anticevic A, Murray JD. Generative modeling of brain maps with spatial autocorrelation. *Neuroimage*. 2020;220:117038.
- 47 Liu X, Wang S, Zhang X, Wang Z, Tian X, He Y. Abnormal amplitude of low-frequency fluctuations of intrinsic brain activity in Alzheimer's disease. *J Alzheimers Dis*. 2014;40(2):387–397.
- 48 Wang K, Liang M, Wang L, et al. Altered functional connectivity in early Alzheimer's disease: a resting-state fMRI study. *Hum Brain Mapp*. 2007;28(10):967–978.
- 49 Sanz-Arigita EJ, Schoonheim MM, Damoiseaux JS, et al. Loss of 'small-world' networks in Alzheimer's disease: graph analysis of fMRI resting-state functional connectivity. *PLoS One*. 2010;5(11):e13788.
- 50 Agosta F, Pievani M, Geroldi C, Copetti M, Frisoni GB, Filippi M. Resting state fMRI in Alzheimer's disease: beyond the default mode network. *Neurobiol Aging*. 2012;33(8):1564–1578.
- 51 Bai F, Watson DR, Yu H, Shi Y, Yuan Y, Zhang Z. Abnormal resting-state functional connectivity of posterior cingulate cortex in amnesic type mild cognitive impairment. *Brain Res*. 2009;1302:167–174.
- 52 Qi Z, Wu X, Wang Z, et al. Impairment and compensation coexist in amnesic MCI default mode network. *Neuroimage*. 2010;50(1):48–55.
- 53 Eyler LT, Elman JA, Hatton SN, et al. Resting state abnormalities of the default mode network in mild cognitive impairment: a systematic review and meta-analysis. *J Alzheimers Dis*. 2019;70(1):107–120.
- 54 Klunk WE, Price JC, Mathis CA, et al. Amyloid deposition begins in the striatum of presenilin-1 mutation carriers from two unrelated pedigrees. *J Neurosci*. 2007;27(23):6174–6184.
- 55 Knight WD, Okello AA, Ryan NS, et al. Carbon-11-Pittsburgh compound B positron emission tomography imaging of amyloid deposition in presenilin 1 mutation carriers. *Brain*. 2011;134(Pt 1):293–300.
- 56 Ryan NS, Keihaninejad S, Shakespeare TJ, et al. Magnetic resonance imaging evidence for presymptomatic change in thalamus and caudate in familial Alzheimer's disease. *Brain*. 2013;136(Pt 5):1399–1414.
- 57 Bick SK, Patel SR, Katnani HA, et al. Caudate stimulation enhances learning. *Brain*. 2019;142(10):2930–2937.
- 58 Albers MW, Gilmore GC, Kaye J, et al. At the interface of sensory and motor dysfunctions and Alzheimer's disease. *Alzheimers Dement*. 2015;11(1):70–98.
- 59 Ikari Y, Nishio T, Makishi Y, et al. Head motion evaluation and correction for PET scans with 18F-FDG in the Japanese Alzheimer's disease neuroimaging initiative (J-ADNI) multi-center study. *Ann Nucl Med*. 2012;26(7):535–544.
- 60 Satterthwaite TD, Wolf DH, Loughhead J, et al. Impact of in-scanner head motion on multiple measures of functional connectivity: relevance for studies of neurodevelopment in youth. *Neuroimage*. 2012;60(1):623–632.
- 61 Van Dijk KR, Sabuncu MR, Buckner RL. The influence of head motion on intrinsic functional connectivity MRI. *Neuroimage*. 2012;59(1):431–438.
- 62 Hallquist MN, Hwang K, Luna B. The nuisance of nuisance regression: spectral misspecification in a common approach to resting-state fMRI preprocessing reintroduces noise and obscures functional connectivity. *Neuroimage*. 2013;82:208–225.
- 63 Karch CM, Goate AM. Alzheimer's disease risk genes and mechanisms of disease pathogenesis. *Biol Psychiatr*. 2015;77(1):43–51.

- 64 Vonsattel JP, DiFiglia M. Huntington disease. *J Neuropathol Exp Neurol.* 1998;57(5):369–384.
- 65 Zeighami Y, Ulla M, Iturria-Medina Y, et al. Network structure of brain atrophy in de novo Parkinson's disease. *Elife.* 2015;4.
- 66 Wang X, Blanchard J, Grundke-Iqbal I, et al. Alzheimer disease and amyotrophic lateral sclerosis: an etiopathogenic connection. *Acta Neuropathol.* 2014;127(2):243–256.
- 67 Eikelenboom P, Bate C, Van Gool WA, et al. Neuroinflammation in Alzheimer's disease and prion disease. *Glia.* 2002;40(2):232–239.
- 68 Veerhuis R, Boshuizen RS, Familian A. Amyloid associated proteins in Alzheimer's and prion disease. *Curr Drug Targets: CNS Neurol Disord.* 2005;4(3):235–248.
- 69 Tousseyn T, Bajsarowicz K, Sanchez H, et al. Prion disease induces alzheimer disease-like neuropathologic changes. *J Neuropathol Exp Neurol.* 2015;74(9):873–888.
- 70 Li Q, Liu Y, Sun M. Autophagy and Alzheimer's disease. *Cell Mol Neurobiol.* 2017;37(3):377–388.
- 71 Manczak M, Park BS, Jung Y, Reddy PH. Differential expression of oxidative phosphorylation genes in patients with Alzheimer's disease: implications for early mitochondrial dysfunction and oxidative damage. *NeuroMolecular Med.* 2004;5(2):147–162.
- 72 Rhein V, Song X, Wiesner A, et al. Amyloid-beta and tau synergistically impair the oxidative phosphorylation system in triple transgenic Alzheimer's disease mice. *Proc Natl Acad Sci U S A.* 2009;106(47):20057–20062.
- 73 Sun H, Wang Y. A new branch connecting thermogenesis and diabetes. *Nat Metab.* 2019;1(9):845–846.
- 74 Vandal M, White PJ, Tournissac M, et al. Impaired thermoregulation and beneficial effects of thermoneutrality in the 3xTg-AD model of Alzheimer's disease. *Neurobiol Aging.* 2016;43:47–57.
- 75 Preller KH, Burt JB, Ji JL, et al. Changes in global and thalamic brain connectivity in LSD-induced altered states of consciousness are attributable to the 5-HT2A receptor. *Elife.* 2018;7.
- 76 Anticevic A, Hu S, Zhang S, et al. Global resting-state functional magnetic resonance imaging analysis identifies frontal cortex, striatal, and cerebellar dysconnectivity in obsessive-compulsive disorder. *Biol Psychiatr.* 2014;75(8):595–605.
- 77 Robinson JL, Lee EB, Xie SX, et al. Neurodegenerative disease concomitant proteinopathies are prevalent, age-related and APOE4-associated. *Brain.* 2018;141(7):2181–2193.
- 78 Burt JB, Demirtas M, Eckner WJ, et al. Hierarchy of transcriptomic specialization across human cortex captured by structural neuroimaging topography. *Nat Neurosci.* 2018;21(9):1251–1259.